

Near zero thermal expansion in metal matrix composites based on intermediate valence systems: Al/TiC

Shanta Mohapatra, Pili Kumari Sahoo

College of Engineering Bhubaneswar, BPUT, Odisha, India

Abstract:

The goal of this work is to create and characterize a novel class of invar composite materials with nearly zero thermal expansion and useful functional characteristics. Particles of Al/TiC, an intermediate valence system with negative thermal conductivity, are used to achieve this expansion contained within an Al matrix. After hot pressing the Al/TiC -21 vol% composite, it was characterized using X-ray computed tomography, capacitive dilatometry, optical and electron microscopy, and XRD. The sample shows invariant behavior up to about 60 K, with a zero coefficient of thermal expansion value close to 45 K, according to the thermal expansion study. The Turner model's temperature range has expanded by roughly 20 K when compared to pure aluminum. Based on commonly used theoretical models, a quantitative analysis of dilatometric experimental data revealed that the Turner model accurately captured the thermal expansion of the Al/TiC composite.

Introduction

The discovery of invar alloys has led to significant progress in the development of high precision instruments such as mechanical chronometers, metrology devices, valves in engines, etc. Although invar is a registered trade name of Fe-Ni₃₆ alloy, invar behaviour, i.e. extremely low coefficient of thermal expansion (CTE), is not bound to that system alone [1–3]. Classical Fe-based invar alloys exhibit reduced thermal expansion in the magnetically ordered domain below Curie-temperature, while in the paramagnetic state “normal” thermal expansion is recovered [2]. Using *ab initio* calculations, Schilfgarde et al. showed that the anomalous contribution to thermal expansion of iron-nickel alloys results from the relaxation of magnetic structures, in which spins may be canted with respect to the average magnetization direction [4]. Despite the low CTE, Fe-Ni₃₆ alloy does not possess many physical properties essential for applications [5]. At the same time, relatively high CTE values are a common property of the majority of metallic functional materials [6]. To reduce the high thermal expansion

of functional materials, metal matrix composites (MMCs) reinforced with various ceramic particles were developed [7–10]. Reinforcement materials include carbides (e.g., SiC, B₄C), nitrides (e.g., Si₃N₄), oxides (e.g., Al₂O₃, SiO₂) and several others [11]. A major step towards controllable thermal expansion in MMCs was made by the discovery of isotropic negative thermal expansion (NTE) over a wide temperature range in ZrW₂O₈ [12]. NTE fillers such as ZrW₂O₈, Sc₂W₃O₁₂, Y₂W₃O₁₂, which contract upon heating, have been promising candidates for the materials intended to compensate for the positive thermal expansion of functional materials [13–15]. Anomalous NTE in zirconium tungstate and related compounds is driven by coupled rotations of rigid polyhedral units ZrO₆ and WO₄ [12,16]. In the meantime, a large number of NTE materials, in which the underlying reasons for this anomalous behaviour are fundamentally different, have been found. All principal mechanisms of NTE have been well described in the review articles [17–20]. In searching for compounds with a highly anomalous contribution to thermal expansion we should explore the systems, in which the lattice class of materials includes intermediate valence (IV) systems – unique chemical compounds based on the 4f-elements with partially filled, almost localized configurations that are nearly degenerate [21]. The effective size of rare earth ions is strongly affected by the temperature-induced changes in the partial delocalization of the 4f electron shell. Thus, NTE is observed in IV systems, in which the thermally excited state of rare earth ions has a lower atomic volume. Samarium-based IV compounds, such as SmB₆, Sm_{1-x}(Y_x)S, Sm_{2.75}C₆₀, may serve as illustrative examples [22–24]. In these systems samarium has two competing electronic configurations: a non-magnetic Sm²⁺ with the 4f⁶ configuration ($J = 0$, the main term is $7F_0$) and magnetic Sm³⁺ with the 4f⁵ configuration ($J = 5/2$, the main term is $6H_{5/2}$). Since the appearance of an additional electron on the 4f shell effectively shields nuclear charge for outer electrons, the effective size of Sm²⁺ is much larger than that of Sm³⁺. The greater the partial charge transfer between the two electronic configurations, the larger the anomalous contribution to thermal expansion is. This specific feature may be a key to controllable thermal expansion. It is possible to tune the overall thermal expansion of the material, provided that there is a way to adjust the magnitude and the temperature scale of the charge transfer between the two electronic states in the system. Sm-based IV systems are prone to demonstrate tunable effective valence of samarium ions caused either by introducing vacancies in the rare-earth sublattice or by partial chemical substitution of Sm ions by non-magnetic trivalent ions (e. g. Y³⁺, La³⁺) [22,23]. The X-ray absorption near

edge structure (XANES) measurements revealed that the introduction of vacancies in rare-earth sublattice increases the effective Sm valence while the lanthanum doping produces the opposite effect [25]. In terms of thermal expansion, a variation of effective Sm valence results in a shift of CTE minimum on the temperature scale and a change of its depth [22,23,26,27]. Summarizing the above, NTE of the IV systems can be adjusted using several methods. CTE of MMCs reinforced with the particles of IV compounds can be precisely tailored to a specific value depending upon the functional material in use and conditions of application. It should be emphasized that the flexibility in CTE control of the proposed MMCs is much higher than in the classical MMCs, in which the thermal expansion is only defined by the ratio of constituents volume fractions. The fundamental difference between composites based on IV systems and previously studied MMCs is the metallic nature of some IV NTE compounds, which appear better suited for modifying the properties of a metal matrix compared to ceramic NTE materials. The values of NTE in IV systems vary widely although the variation in temperature is limited. NTE values of selected IV systems are listed in Table 1 [28–32]. The temperature range over which the IV systems based on Sm and Yb display NTE imposes restrictions on the invar region of composites. Namely, one should expect operation at temperatures below room temperature. This limitation is not dramatic, since the operating temperatures of many applications, for example the aerospace or cryogenic technologies, lie mainly within the range of low temperatures. Simple structural materials whose only advantages are mechanical properties and dimensional stability when heated or cooled are out of discussion. In turn we are trying to contribute to the progress in the development of materials with unique combinations of functional properties (electronic/ magnetic/ thermodynamic/ transport/ optical) with a specified limit on the CTE value. This research explored the characterization of microstructure and thermal expansion behaviour of the first developed MMCs reinforced with the particles of an IV system. We aimed to decrease the CTE of Al, a widely used functional material, to near zero value at certain temperature by adding particles of classical IV system with NTE – SmB₆. Although the contraction of SmB₆ is not the highest among IV systems and is limited by low temperatures, the use of this compound as NTE filler can be beneficial due to its high chemical stability and high melting point, which prevent chemical reaction with the metal matrix. Another important point is the commercial availability of samarium hexaboride. Readers who are

interested in higher temperatures or need larger NTE values can refer to Table I or review articles [17,19].

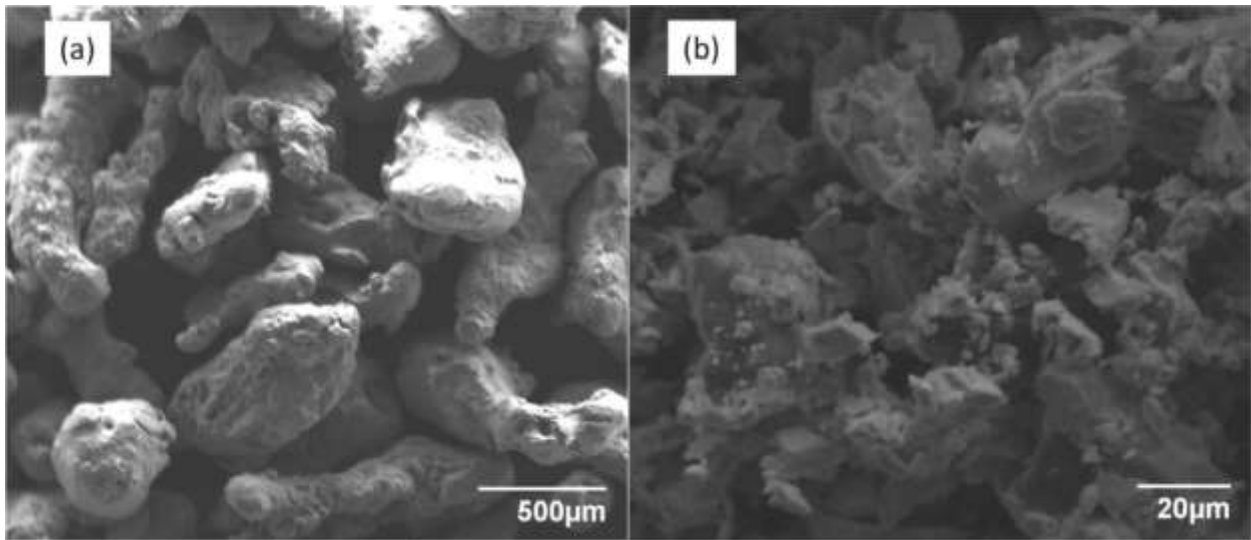


Fig. 1. SEM image of Al (a) and SmB6 (b) powders

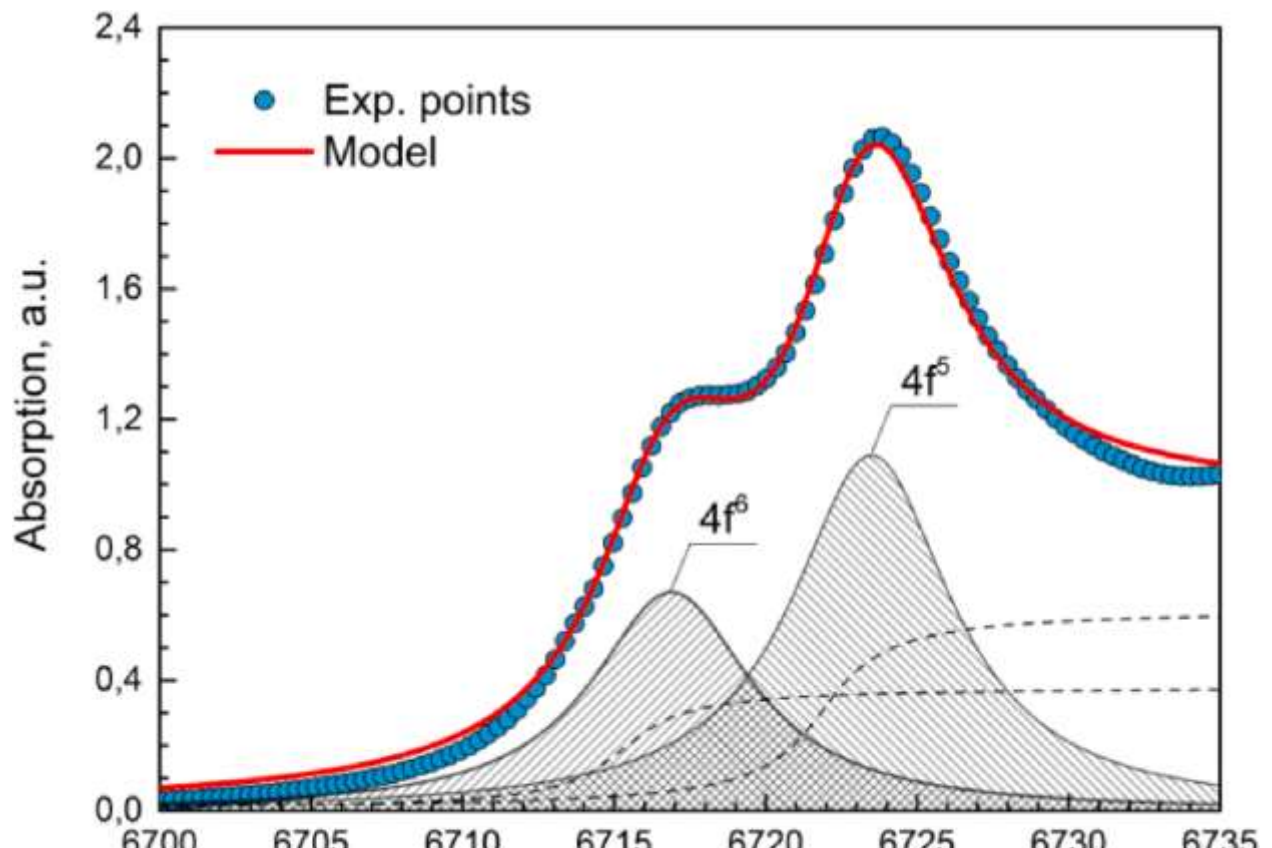


Fig. 2. Sm L3-edge absorption spectra of SmB6 at 300 K.

In this article, we would like to present the results of the study of Al/ SmB6 composite fabricated by hot pressing powder blends. The sample has been examined by optical and electron microscopy, X-ray tomography, and X-ray diffraction. Thermal expansion of Al/SmB6 composite has been measured by capacitive dilatometry and analyzed using various theoretical models to single out the best model for CTE description in novel metal/metal composite.

Experimental methods and techniques

Composite preparation

Commercially available Al powder (UC Rusal, 99.5% purity, size < 0.5 mm) and SmB6 powder (Haihang Industry Co., Ltd, 99.9% purity, size < 20 μm) were used for the study (Fig. 1a and b respectively). In the beginning, Al powder was ball milled in a PULVERISETTE 6 (Fritsch, Germany) planetary ball-mill through the use of ceramic ZrO₂ milling balls with a diameter of 8 mm and a ball-to-powder weight ratio of 15:1. Ball milling was carried out for 15 min with the revolving speed 400 rpm. After that SmB6 powder were weighed and mixed with finely powdered aluminum with the mass ratios of 1:2, which corresponding to SmB6-21 vol%. According to the Turner model this mass ratio meet a requirement of near zero CTE of Al/SmB6 composite at $T = 40 \text{ K}$, i.e. the temperature at which SmB6 exhibits the largest NTE. Powder blend were then high-energy ball milled for 10 min under the same conditions. The resulting mixture of Al/SmB6 powders was hot pressed in a special heated steel die at 450 °C under an applied pressure of 350 MPa to obtain a compact with a diameter of 17 mm and a height of 10 mm.

Characterization

The surface morphology of initial Al and SmB₆ powders, Al/SmB₆ powder blend and bulk composite was imaged using a JEOL JSM- 6390LV scanning electron microscope (SEM). The X-ray absorption near edge structure (XANES) measurements near the Sm L₃-edge were carried out for SmB₆ at the STM beam line of Kurchatov synchrotron radiation source KISI at room temperature to experimentally confirm the IV state of Sm ions. The Al and SmB₆ powders, Al/SmB₆ powder blend and Al/SmB₆ bulk composite were characterized by X-ray diffraction (XRD) using synchrotron-generated X-Ray beam with $E = 15.2$ keV ($\lambda = 0.826$ Å) at STM beamline of KISI source and using laboratory X-ray source BRUKER D8 ADVANCE with $E = 8.04$ keV ($\lambda = 1.541$ Å). The distribution of SmB₆ particles within an Al matrix in the fabricated Al/SmB₆ composite was analyzed by optical microscopy (Leica DM ILM) on the polished surfaces. The microstructure of the entire volume of the sample was studied by X-ray computed tomography (Y. Cheetah YXLON X-ray inspection system). In contrast to classical methods for microstructure characterization, such as optical or electron microscopy, which require preliminary sample cutting, etching and polishing, X-ray tomography is a non-destructive tool for internal structure diagnostic of the entire volume of the sample. Using slice-to-slice technology X-ray computed tomography reconstructs 3D models from a set of 2D X-ray images with a high resolution (up to 2 μm). Thermal expansion measurements of Al/SmB₆ composite were carried out at Kirensky Institute of Physics by capacitive dilatometry using a hand-made measuring cell/option installed in the PPMS (Quantum Design) system (for more details see [33]) in the temperature range 10–210 K.

Experimental results

XANES

The experimental spectrum in Fig. 2 displays two characteristic peaks corresponding to the integer valent states: divalent 4f⁶ state and trivalent 4f⁵ state of Sm atom. The absorption line shapes were analyzed using a deconvolution technique presented in [34]. Using a set of Lorentzian and arctangent functions representing the core-hole lifetime width and the transitions into the continuum states respectively, we fit the following expression to the experimental spectrum:

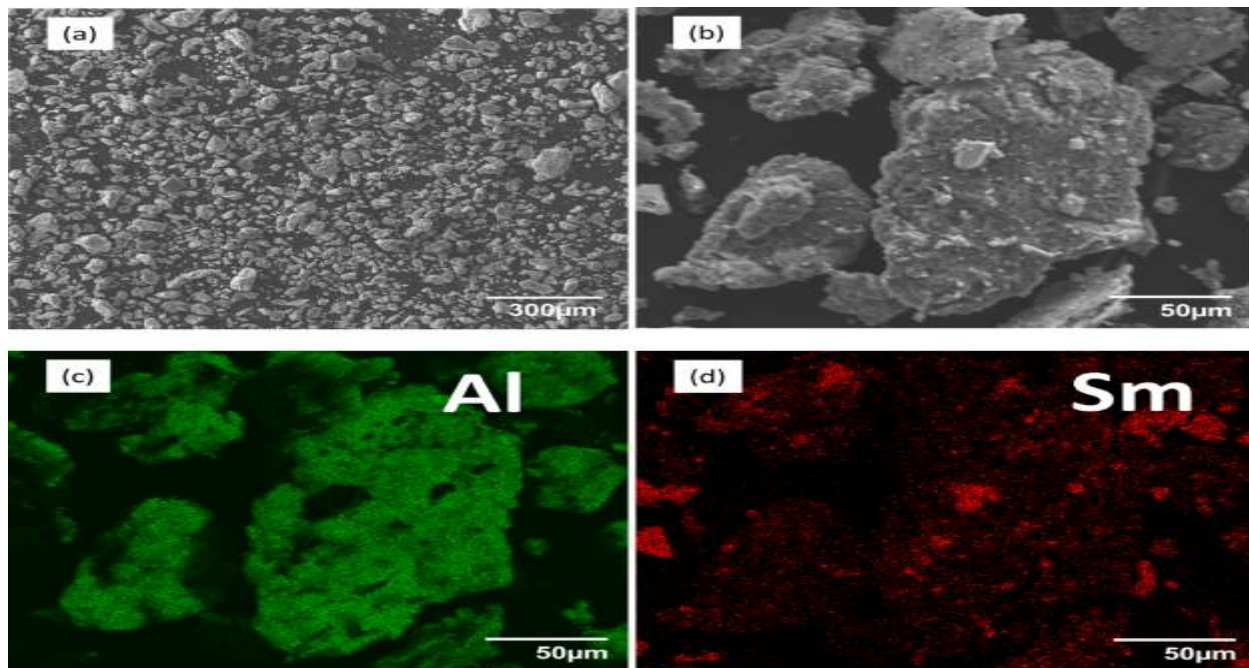


Fig. 3. SEM images of TiC powder blend (*a, b*) and EDS elemental mapping (*c, d*).

Microstructure and XRD

Fig. 3 shows the SEM images of Al/SmB₆ powder blend and EDS

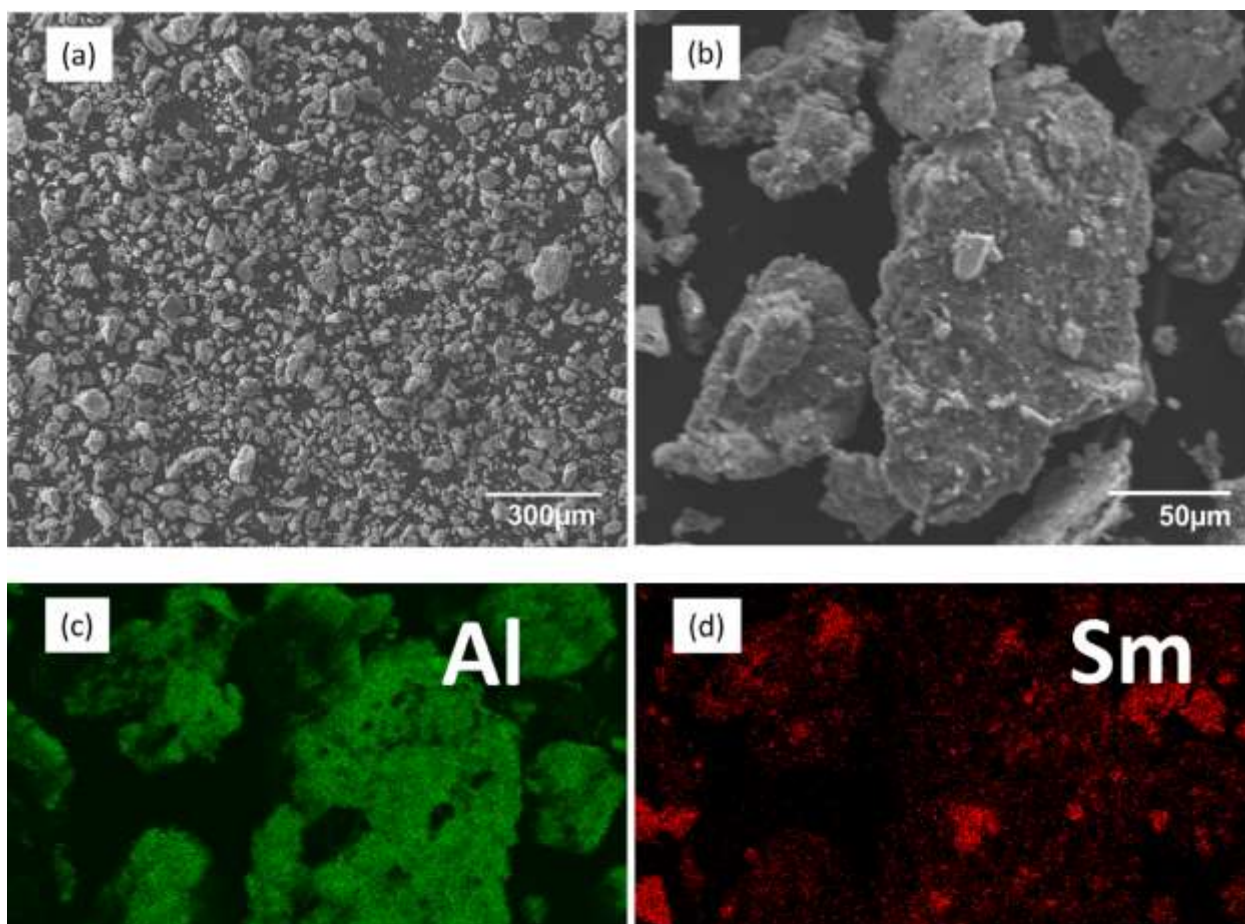


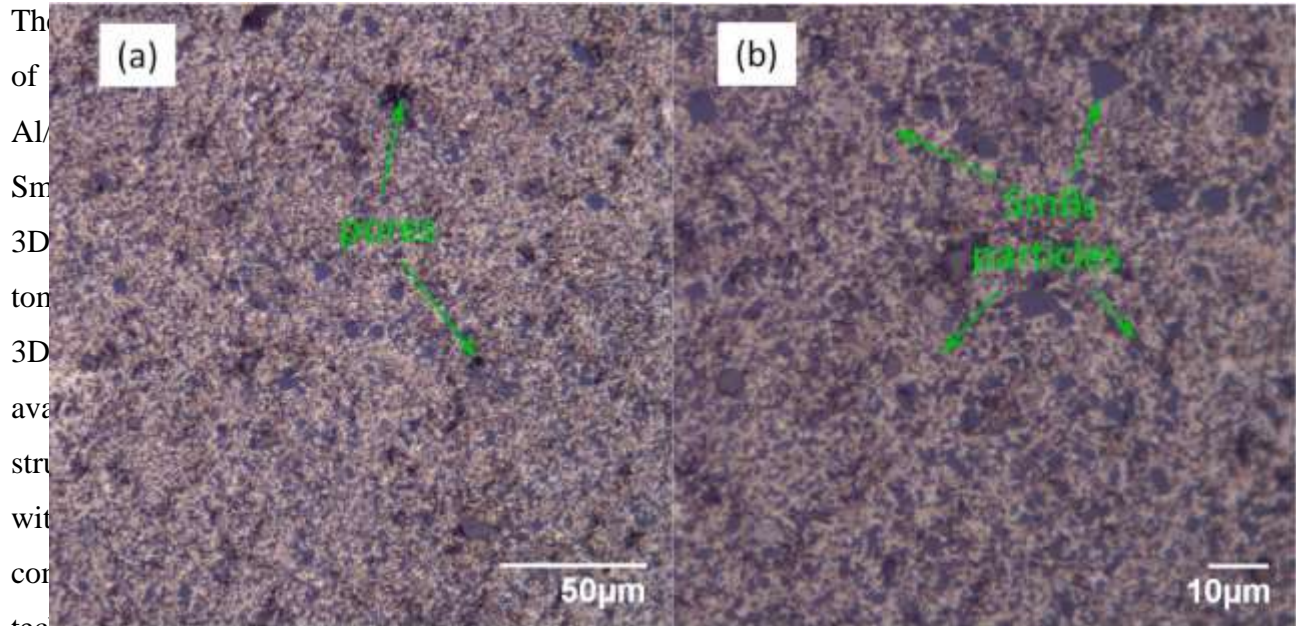
Fig. 3. SEM images of Al/SmB₆ powder blend (*a, b*) and EDS elemental mapping (*c, d*).

Here E is the photon energy, B_0 and B_1 denote linear background. The strengths of the individual Lorentzian line shapes are given by p_1 and p_2 , while a half-width at full maximum Γ denotes the lifetime of electron excitation from 2p-core level to an empty 5d-states. The δ value corresponds to a shift of the continuum of ≈ 1.6 eV as observed in Sm-based compounds [35]. As a result of fitting procedure we extracted the independent parameters $p_1 = 0.67$, $p_2 = 1.09$ and $\Gamma = 3.2$ eV. The ratio of amplitudes p_1/p_2 , expressing the effective intermediate valence $Sm^{+2.61}$, is in a good agreement with that reported earlier for SmB₆ [36].

Microstructure and XRD

Fig. 3 shows the SEM images of Al/TiC powder blend and EDS elemental mapping (the map for light B atoms is omitted since it's less indicative than the map for Sm atoms with high Z number). As can be seen from the Fig. 3a, the size of the particles doesn't exceed 150 μm . The resulting mixture consists of Al + SmB₆ agglomerates and SmB₆ particles (Fig. 3b,c,d). Agglomerates present micro- and sub-micron particles of samarium hexaboride embedded in aluminum matrix. Agglomerates are characterized by an irregular shape with a developed surface morphology. In contrast, SmB₆ particles can be identified by the smooth chipping surfaces, typical of brittle materials. Typical optical micrographs of Al/SmB₆ bulk composite are depicted in Fig. 4a,b. The results indicate that samarium hexaboride particles are dispersed homogeneously within the aluminum matrix and their size doesn't exceed 20 μm . Negligible pores with a size less than 5 μm are also observed in Fig. 4a, formation of which usually accompanies the polishing procedure. It should be noted that some pores may have remained

after the pressing process, nevertheless their size and volume fraction are negligible and can't affect the thermodynamic properties of the sample significantly. The XRD patterns of Al and SmB6 powders, Al/SmB6 powder blend and Al/SmB6 bulk composite are presented in Fig. 5.



technology (Fig. 7). As can be seen from the image, a granular structure has formed near one of the two plane-parallel faces of the sample probably due to powders segregation at the mixing stage. From the above, it can be inferred that the manufacturing route and the process conditions for a fabrication of the composite under consideration were selected properly.

Fig. 4. Optical micrographs of Al/SmB₆ composite.

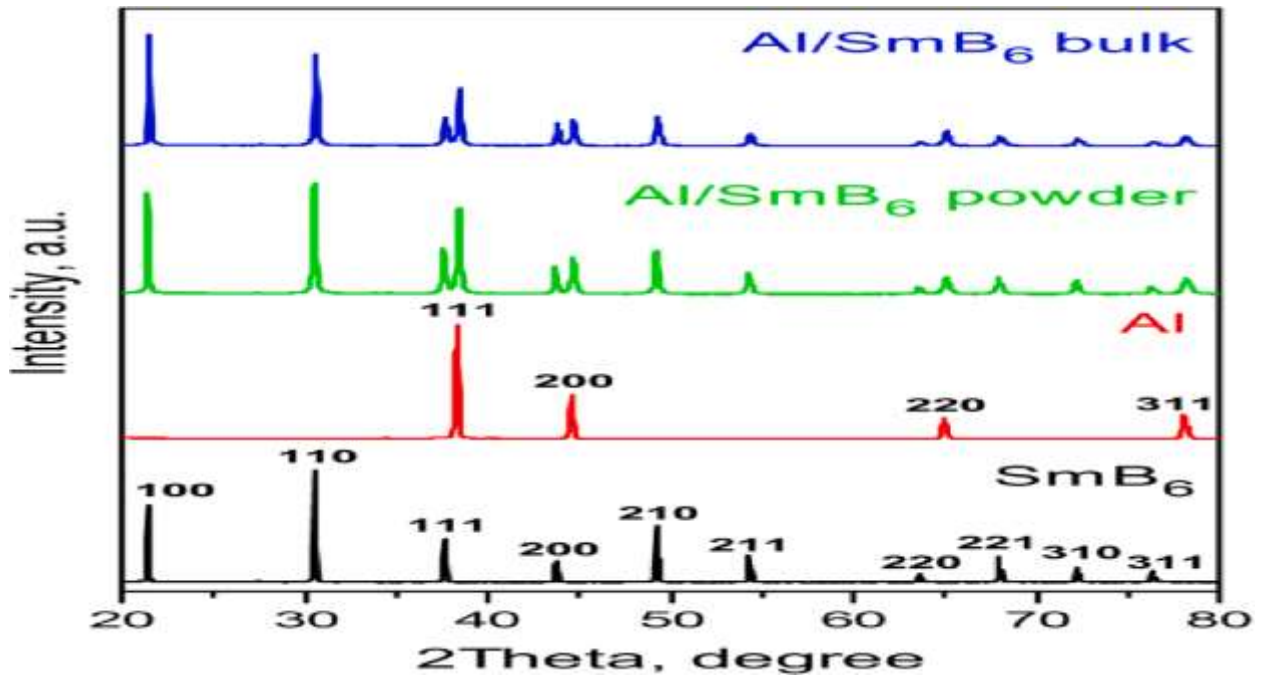


Fig. 5. XRD patterns of Al and SmB₆ powders, Al/SmB₆ powder blend and Al/ SmB₆ composite

Coefficient of thermal expansion

The relative thermal expansion of Al/SmB₆ composite measured by capacitive dilatometry using a hand-made measuring cell/option installed in the PPMS (Quantum Design) system is shown in Fig. 8a. Since the cell material also expands upon heating, this contribution to thermal expansion was defined and extracted through the capacitance measurements of silver with 99.99% purity, the CTE values of which are well known [37,38]. It's worth noting that we performed repeated measurements, which showed identical results, to make sure that a

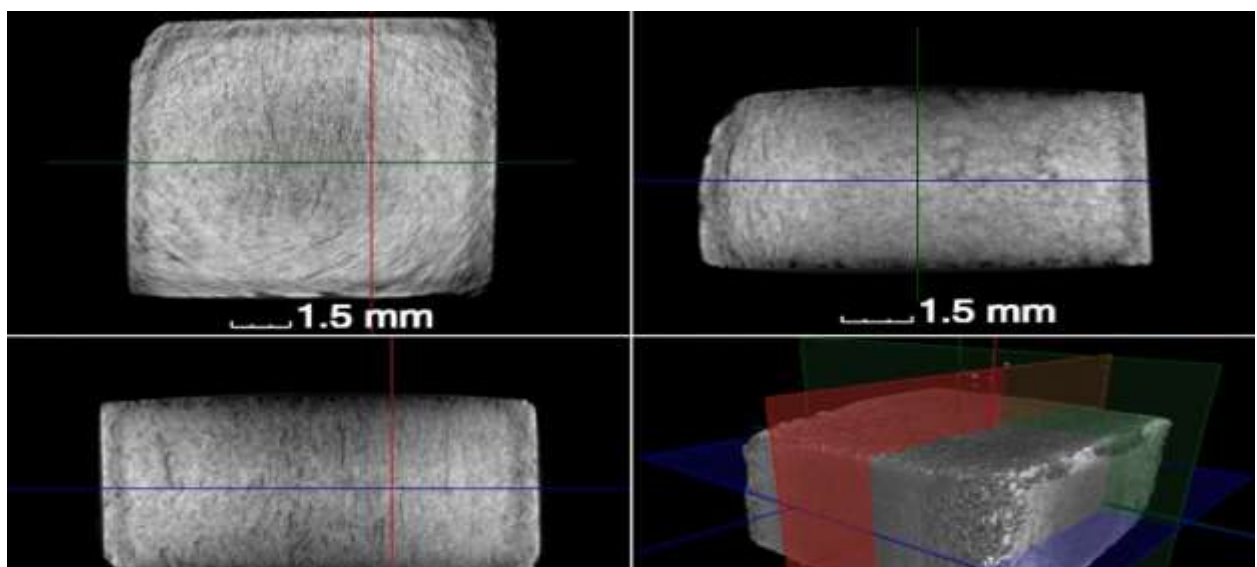


Fig. 6. X-ray 2D-sections in three basic planes and a 3D X-ray micro tomographic reconstruction of Al/SmB6 composite. Color palette is inverted, i.e. the black color indicates the regions without absorption of X-rays.

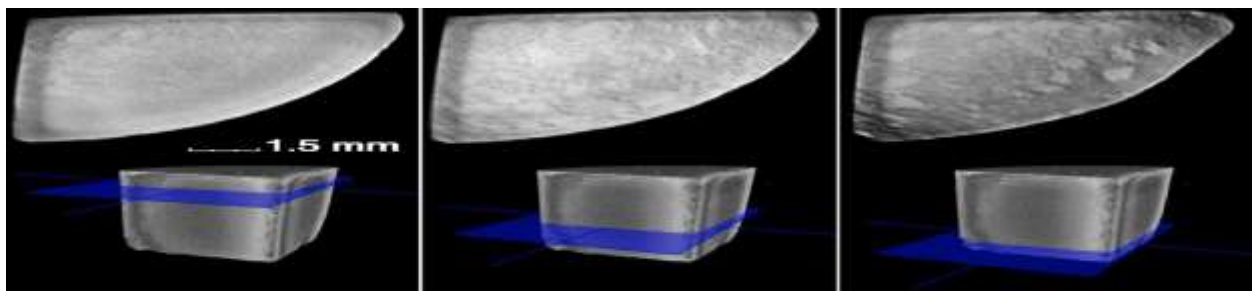


Fig. 7. X-ray cross-sections at varying heights of the second Al/SmB6 composite manufactured using a

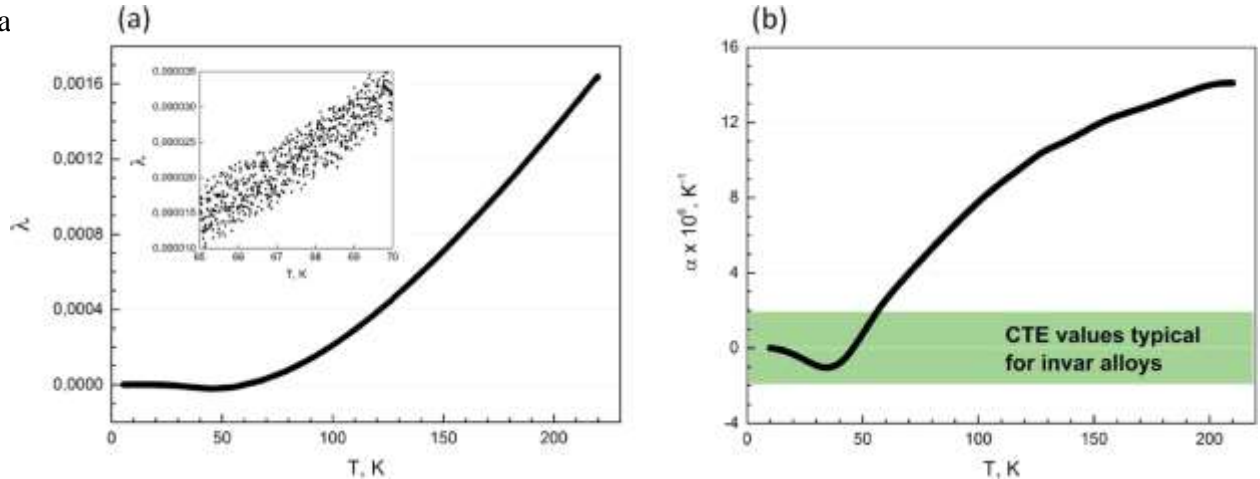


Fig. 8. Relative thermal expansion (a) and linear CTE (b) of Al/SmB6 composite in the temperature range 10–210 K. The inset indicates a spread of values.

probable stress relaxation doesn't affect the experimental curve (such physical picture was observed in [13] for example). In Fig. 8b we show the experimental results of the linear CTE of Al/ SmB6 composite obtained by taking derivatives $d\lambda/dT$. To prevent oscillations of the CTE

function, the dependence $\lambda(T)$ were preliminarily smoothed using the spline function. Below ~ 45 K, α is negative, while at higher temperatures α then becomes positive. Filled area on Fig. 8b indicates that the sample exhibits invar behaviour, i.e. CTE values less than $|2| \times 10^{-6} \text{ K}^{-1}$, at temperatures up to ~ 60 K. In comparison to pure aluminum, the temperature range has increased by about 20 K. The temperature range of invar-like behaviour (0–60 K) may seem rather narrow for practical applications. In particular, it is lower than the boiling point of liquid nitrogen $T = 77$ K, which closes many potential niches for the developed material. In our case, we are not trying to compete with classical Fe-Ni alloys in their well-known application. On the contrary, the motivation was to develop invar materials of a new type and test the principle. For instance, the thermal conductivity of classic Fe-Ni36 invar alloy is almost 20 times lower comparing to p aluminum [39]. In this way, the developed Al/SmB6 composite may possess a unique combination of useful functional properties inherent in the matrix material, and a specified limit on the CTE value.

Discussion To develop composites with predetermined properties, such as the thermal expansion, it is very important to base on a reliable model capable of predicting CTE of the composite. Those models that worked well for ceramic-based MMCs may be less efficient for the systems under study. The point is that SmB6, the compound that belongs to the class of higher borides, differs greatly in its physical properties from complex oxides and ceramic materials. The composites studied in this work can be considered as systems based on metal components excepting the region of the lowest temperatures. Pure SmB6 is a narrow-gap insulator (Kondo insulator), but at temperatures above several tens of degrees, the electrical conductivity becomes metallic. Any inhomogeneities and impurities reduce the size of the gap in the density of the electronic states of

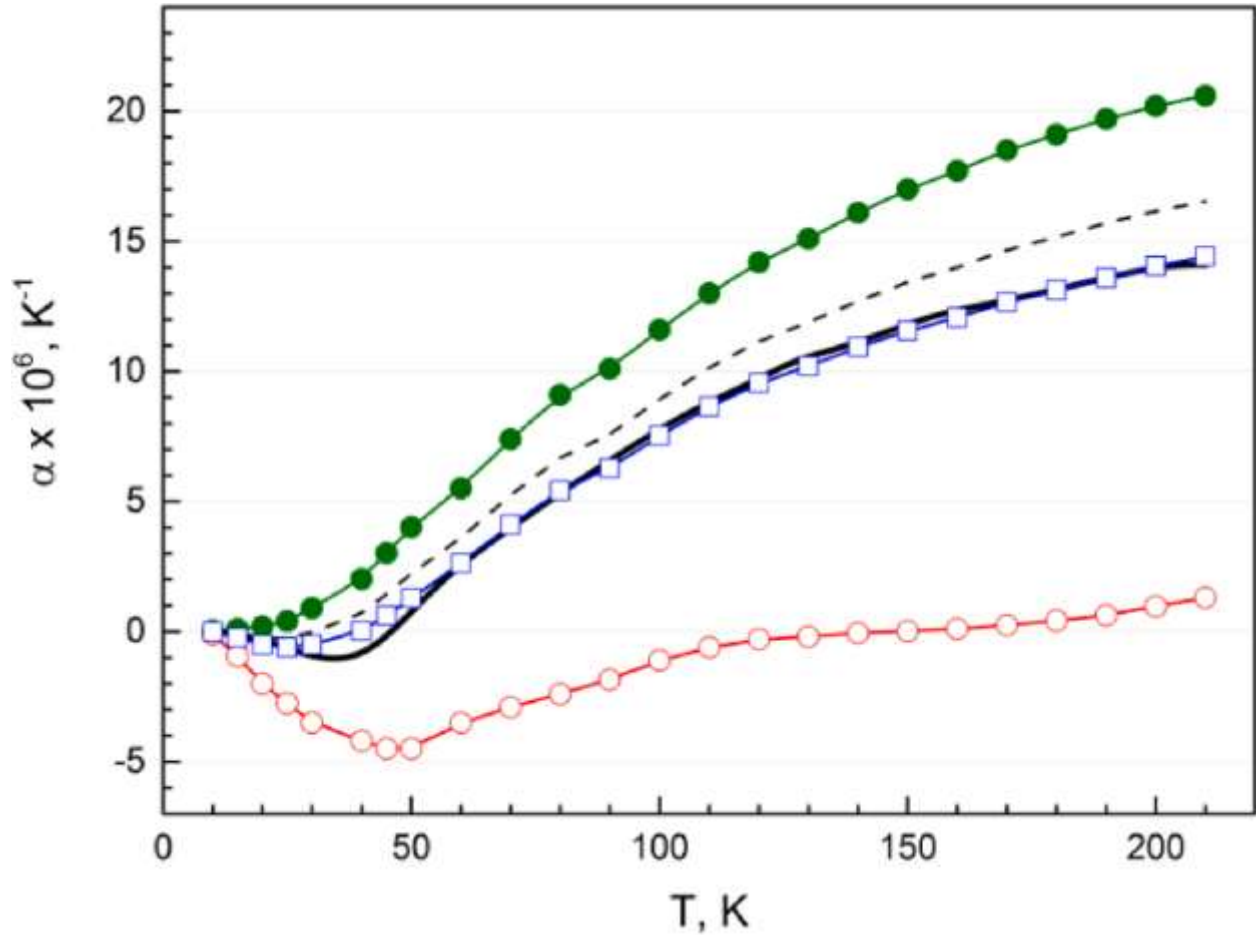


Fig. 9. Plot of experimental CTE values (black solid line) along with curves representing CTE values calculated using thermo-elastic models for the Al/ SmB6 composite. Green filled circles – CTE of Al; red open circles – CTE of SmB6; dashed line – results of the ROM model assuming SmB6-21 vol%; blue open squares – results of the ROM, Ternner and Kerner models assuming various volume fractions, see text for details. (For interpretation of the references to color in this figure legend, the reader is referred to the web version of this article.)

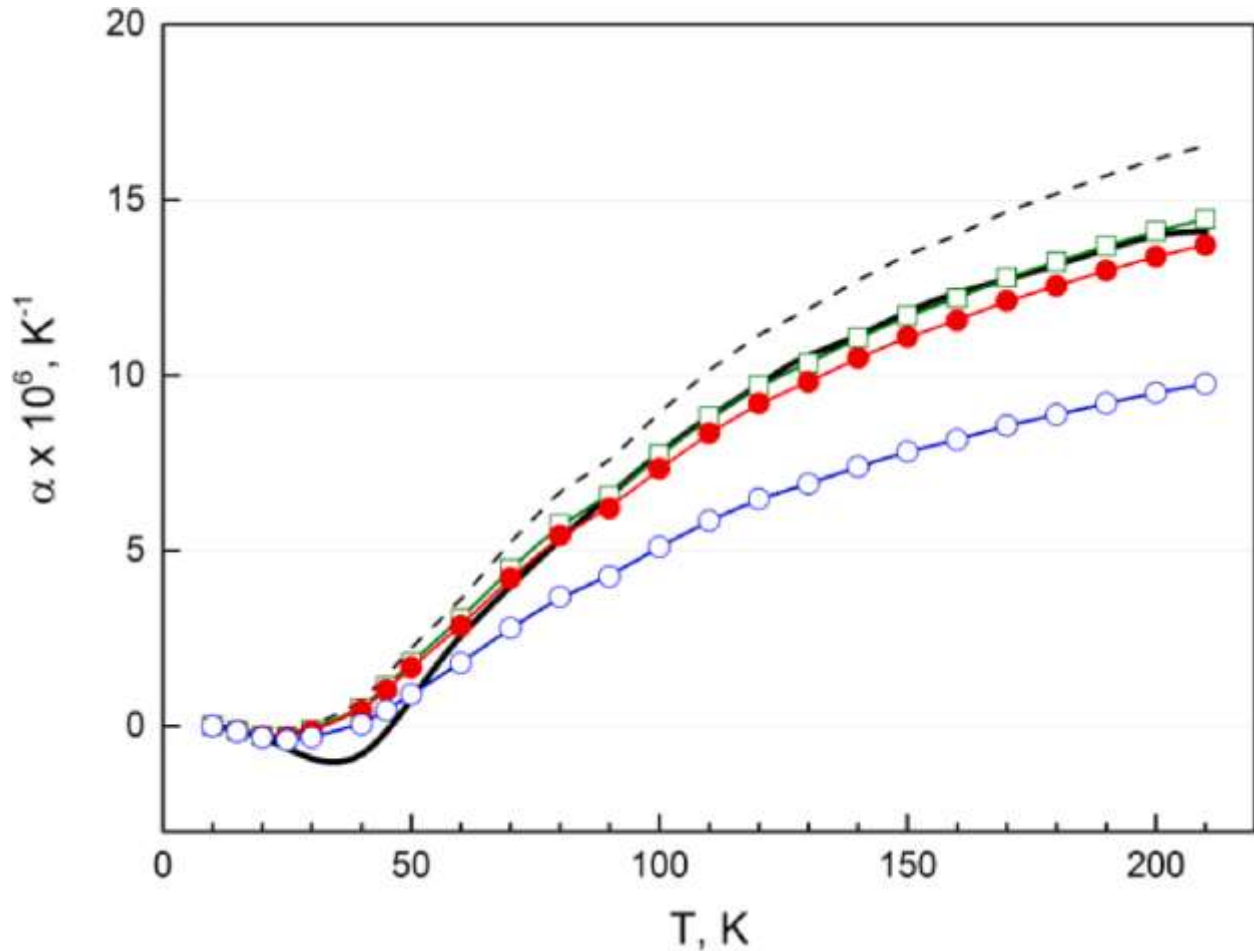


Fig. 10. Plot of experimental CTE values (black solid line) along with curves representing CTE values calculated using the EROM model for the Al/SmB6 composite N°1. Dashed line – results of the classic ROM model assuming SmB6-21 vol%. Symbols – results of the EROM model assuming: $\alpha_{in} = \alpha_{Al}/3$ and $\Delta = 2 \mu\text{m}$ (green squares), $\alpha_{in} = \alpha_{Al}/10$ and $\Delta = 2 \mu\text{m}$ (red filled circles), $\alpha_{in} = \alpha_{Al}/10$ and $\Delta = 4 \mu\text{m}$ (blue open circles). (For interpretation of the references to color in this figure legend, the reader is referred to the web version of this article.)

As shown in this section, the Turner model is well-suited for CTE description of Al/SmB6 composite over a very wide temperature range. We assume that it will remain reliable for the composites based on doped (modified) samarium hexaboride. However, this assumption should be confirmed by the forthcoming studies. It should be noted that we relied on literature data on the elastic properties of SmB6. In the case of doped borides, in order to use the Turner model one should either measure the elastic properties of the IV component or use model assumptions on the value of the bulk modulus.

Conclusions

This study represents the first experimental investigation of the metal matrix composite's microstructure and thermal expansion behavior based on the intermediate valence system. We created a composite using the hotpressing method that included SmB6-21 vol%, a traditional intermediate valence system with negative thermal expansion, and Al-79 vol%, a functional material that is widely used. The values of negative thermal expansion in intermediate valence systems can be changed, in contrast to ceramic NTE fillers like ZrW₂O₈, by adding vacancies to the rare-earth sublattice or by partially substituting 4f-elements with partially From this perspective, intermediate valence systems with NTE are better suited for modifying the thermal expansion of a metal matrix compared to ceramics with strictly specified NTE values

The Al/SmB6 composite was evaluated using optical, XRD, and X-ray computed tomography and electron microscopy. The latter method produces a 3D volumetric model that displays the distribution of SmB6 particles. was rebuilt within an Al matrix. Capacitive dilatometry measurements of the sample's thermal expansion showed that it exhibited invar behavior, with CTE values less than $2 \times 10^{-6} \text{ K}^{-1}$ up to $\sim 60 \text{ K}$ and a zero coefficient of thermal expansion value close to 45 K . There has been a 20 K increase in temperature range when compared to pure aluminum. The thermal expansion of the Al/SmB6 composite was accurately simulated by the Turner model, according to a quantitative study of dilatometric experimental data conducted using commonly used theoretical models.

CRedit authorship contribution statement

D.A. Serebrennikov: Investigation, Writing - original draft. A.A. Bykov: Investigation, Writing - review & editing. A.L. Trigub: Investigation. N.A. Kolyshkin: Investigation, Writing - review & editing. A.L. Freydmann: Investigation, Writing - review & editing. A.V. Aborkin: Investigation, Writing - original draft. A.O. Tovpinets: Investigation, Writing - review & editing. E.S. Clementyev: Conceptualization, Writing - original draft. A.Yu. Goikhman: Supervision, Funding acquisition, Writing - review & editing.

Declaration of Competing Interest

The authors declare that they have no known competing financial interests or personal relationships that could have appeared to influence the work reported in this paper.

Acknowledgements

This work was supported by the Russian Foundation for Basic Research, grant 18-32-00583 mol_a and by the State assignment of Russia, project FZWM-2020-0008. We are grateful to V.N. Leitsin for his support in the experimental studies.

Appendix A. Supplementary data

Supplementary data to this article can be found online at <https://doi.org/10.1016/j.rinp.2021.103843>.

References

- [1] Wasserman EF. Acet M. Invar, Anti-Invar: Magnetovolume Effects in Fe-Based Alloys Revisited. In: Planes A., Manosa L., Saxena A., editors. Magnetism and Structure in Functional Materials. Berlin, Heidelberg: Springer, 177; 2005.
- [2] Shiga M. *Curr Opin Solid State Mater Sci* 1996;1:340.
- [3] Wasserman EF. INVAR: Moment-volume instabilities in transition metals and alloys. In: Buschow, K. H. J. & Wohlfarth, E., editors. *Ferromagnetic Materials Vol. 5*. Amsterdam: North-Holland, 237; 1990.
- [4] Schilfgaard M, Abrikosov IA, Johansson B. *Lett Nat* 1999;400:46.
- [5] Sidhu SS, Kumar S, Batish A. *Crit Rev Solid State Mater Sci* 2016;41:132.
- [6] Wu D, Wu S-P, Yang L, Shi C-D, Wu Y-C, Tang W-M. *Powder Metall* 2015;58:100.
- [7] Nam TH, Requena G, Degischer P. *Compos A* 2008;39:856.
- [8] Shu K-M, Tu GC. *Mater Sci Eng, A* 2003;349:236.
- [9] Xue ZW, Wang LD, Liu Z, Fei WD. *Scr Mater* 2010;62:867.
- [10] Elomari S, Skibo MD, Sundarrajan A, Richards H. *Compos Sci Technol* 1998;58: 369. [11] Ibrahim IA, Mohamed FA, Lavernia EJ. *J Mater Sci* 1991;26:1137.
- [12] Mary TA, Evans JSO, Vogt T, Sleight AW. *Science* 1996;272:90.
- [13] Holzer H, Dunand DC. *J Mater Res* 1999;14:780.

- [14] Gao S, Zhao N, Liu Q, et al. *J Alloys Compd* 2019;779:108.
- [15] Sa Das, Si Das, Das K. *Ceram Int* 2014;40:6465.
- [16] Sleight AW. *Ann Rev Mater Sci* 1998;28:29.
- [17] Chen J, Hu L, Deng J, Xing X. *Chem Soc Rev* 2015;44:3522.
- [18] Evans JSO. *J Chem Soc, Dalton Trans* 1999;19:3317.
- [19] Barrera GD, Bruno JAO, Barron THK, Allan NL. *J Phys: Condens Matter* 2005;17: R217.
- [20] Takenaka K. *Sci Technol Adv Mater* 2012;13:013001.
- [21] Riseborough RS, Lawrence JM. *Rep Prog Phys* 2016;79:084501.
- [22] Nefedova EV, Alekseev PA, Klement'ev ES, Lazukov VN, Sadikov IP, Khlopin MN, Tsetlin MB, *JETP* 88, 565; 1999.
- [23] Alekseev PA, Mignot J-M, Nefedova EV, et al. *Phys Rev B* 2006;74:035114.
- [24] Arvanitidis J, Papagelis K, Margadonna S, Prassides K, Flitch AN. *Nature* 2003;425: 599.
- [25] Gabani S, Flachbart K, Bednarcik J, Welter E, Filipov V, Shitsevalova N. *Acta Phys Pol A* 2014;126:338.
- [26] Nefedova EV, Alekseev PA, Lazukov VN, Sadikov IP. *JETP* 2003;96:1113.
- [27] Serebrennikov DA, Clementyev ES, Alekseev PA. *J Magnetism Magnetic Mater* 2019;470:131.
- [28] Margadonna S, Arvanitidis J, Papagelis K, Prassides K. *Chem Mater* 2005;17:4474.
- [29] Kuznetsov AYU, Dmitriev VP, Bandilet OI, Weber H-P. *Phys Rev B* 2003;68:064109.
- [30] Hauser R, Ishii T, Uwatoko Y, Oomi G, Bauer E, Gratz E. *JMMM* 1996;157/158: 679.
- [31] Pott R, Schefzyk R, Wohlleben D, Junod AZ. *Phys B - Condensed Matter* 1981;44: 17.
- [32] Uwatoko Y, Oomi G, Thompson JD, Canfield PC, Fisk Z. *Phys B* 1993;186–188:594.
- [33] Freidman AL, Popkov SI, Semenov SV, Turchin PP. *Tech Phys Lett* 2018;44:123.

- [34] Rohler J. JMMM 1985;47&48:175.
- [35] Deen PP, Braitwaite D, Kernavanois N, et al. Phys Rev B 2005;71:245118.
- [36] Mizumaki M, Tsutsui S, Iga F. J Phys Conf Ser 2009;176:012034.
- [37] White GK, Collins JG. J Low Temp Phys 1972;7:43.
- [38] K uchler R, Bauer T, Brando M, Steglich F. Rev Sci Instrum 2012;83:095102.
- [39] Babichev AP, Babushkina NA, Bratkovskiy AM, et al., In: Grigorieva I.S., Mejlihova E.Z., editors. Physical values. Moscow: Energoatomizdat, 1232; 1991.
- [40] Hsien CL, Tuan WH. Mater Sci Eng, A 2007;460–461:453.
- [41] Kozhevnikov IG, Novitskiy LA. In: Gordov A.N., editor. Teplofizicheskie svoistva materialov pri nizkih temperaturah. Moscow: Mashinostroenie, 98; 1982.
- [42] Nakamura S, Goto T, Kunii S, Iwashita K, Tamaki A. J Phys Soc Jpn 1994;63:623.
- [43] Archer RR, Cook NH, Crandall SH. et al. In: Clark BJ, editor. An introduction to the mechanics of solids. New York: McGraw-Hill Inc.; 1978. p. 286.
- [44] Park C-S, Kim M-H, Lee C. J Mat Sci 2001;36:3579. [45] Gonzalez-Benito J, Castillo E, Caldito JF. Eur Polym J 2013;49:1747.